A Letters Journal Exploring the Frontiers of Physics

October 2012

EPL, **100** (2012) 28004 www.epljournal.org
doi: 10.1209/0295-5075/100/28004

The size, shape, and dynamics of cellular blebs

F. Y. Lim[1], K.-H. Chiam[1,2] and L. Mahadevan[3(a)]

[1] *A*STAR Institute of High Performance Computing - 1 Fusionopolis Way, #16-16, Singapore 138632, Singapore*
[2] *Mechanobiology Institute, National University of Singapore - 5A Engineering Drive 1, Singapore 117411, Singapore*
[3] *School of Engineering and Applied Sciences, Department of Physics, Harvard University 29 Oxford Street, Cambridge, MA 02138, USA*

received 15 September 2012; accepted 28 September 2012
published online 31 October 2012

PACS 87.16.Qp – Pseudopods, lamellipods, cilia, and flagella
PACS 87.17.Aa – Modeling, computer simulation of cell processes
PACS 87.17.Rt – Cell adhesion and cell mechanics

Abstract – A cellular bleb grows when a portion of the cell membrane detaches from the underlying cortex under the influence of a cytoplasmic pressure. We develop a quantitative model for the growth and dynamics of these objects in a simple two-dimensional setting. In particular, we first find the minimum cytoplasmic pressure and minimum unsupported membrane length for a stationary bleb to nucleate and grow as a function of the membrane-cortex adhesion. We next show how a bleb may travel around the periphery of the cell when the cytoplasmic pressure varies in space and time in a prescribed way and find that the traveling speed is governed by the speed of the pressure change induced by local cortical contraction while the shape of the traveling bleb is governed by the speed of cortical healing. Finally, we relax the assumption that the pressure change is prescribed and couple it hydrodynamically to the cortical contraction and membrane deformation. By quantifying the phase space of bleb formation and dynamics, our framework serves to delineate the range and scope of bleb-associated cell motility.

Introduction. – Blebs are protrusions of a cell membrane driven by local variations in intracellular pressure induced by contractility and are commonly seen in many types of cells. Blebbing is closely related to an elementary mechanical process —the formation of a blister in a thin film adherent to a substrate, but also rather different in that it involves a number of active processes: active (and regulated) contractile stresses that drive the process, as well as active mechanisms associated with bleb healing via forces at the boundary. Cellular blebbing is an important mechanism contributing to apoptosis, cytokinesis, and cell motility in normal and pathological/cancer cells [1–6]. In the context of motility, recent experiments [7,8] on various cell types show that blebs arise as a result of homogenous intracellular pressure change coupled with a global contraction of the entire cytoskeleton. It has been further suggested that bleb protrusions can cooperate with lamellipodium-based protrusions to power cell motility [2,5], and cells can switch between different motility modes depending on their environment [4,6,9,10]. Thus the focus on actin polymerization-driven protrusions in lamellipodia and filopodia on cell motility must be complemented by considerations of contractility/pressure induced blebbing before one can determine the relative contributions of these modes for whole cell motility. Understanding blebbing quantitatively is a first step in this process.

While there have been some previous theoretical studies [11,12] on aspects of blebbing such as for formation time or growth, here we focus on a synthetic approach that accounts for the nucleation, expansion, retraction, and large scale movements of blebs, with the aim of providing a qualitative theory presented as a series of phase diagrams. A bleb is nucleated when the local hydrostatic pressure generated by cortical contraction causes the cell membrane to detach from the cortex. Cytoplasmic pressure and flow then drive the expansion of a bleb. This is accommodated by further delamination of the cell membrane from the cortex, flow of lipid into the bleb through the bleb neck, and unwrinkling of excess folded membrane. Eventually, the bleb expansion slows down as the driving contractile pressure is relieved, and the actin cortex starts to reform underneath the bleb membrane and the bleb heals. In non-motile cells, myosin-driven

(a) E-mail: lm@seas.harvard.edu (corresponding author)

contraction of the reformed cortex retracts the bleb, while in motile cells, contraction of the rear of a cell leads to a net movement of the cell body towards the leading edge where the bleb is formed. Sometimes an asymmetric reformation of the actin cortex leads to bleb movements around the periphery of a cell [13]. During this last process, the actin cortex is reformed asymmetrically on one side of the bleb and its contraction pushes the cytosol to the other side of the bleb, leading to delamination of the membrane on the unconsolidated edge, and thence motion.

Model. – To quantify these phenomena, we focus on a simple 2-dimensional model of the dynamics of a cell, consisting of an active fluid —a contractile cortex bathed in a Newtonian fluid, and surrounded by a membrane that is detachable from the actin cortex. While our model can be extended to three dimensions, here we limit ourselves to the simplest geometry where we still can capture many of the qualitative trends. We assume that the membrane is one-dimensional and neglect its natural curvature, which is reasonable for blebs that are small compared with the size of the cell. In addition, we focus on a single bleb and thus neglect bleb-bleb interactions, as well as the adhesion of the bleb to any external scaffolds or substrates. For a single bleb, denoting the distance between the detached membrane and the cortex as $y(x)$ at the position x, the energy per unit width $E(x, y, y_x, y_{xx})$ of a piece of blistered membrane $y(x)$ is given by

$$E = \int_{s_l}^{s_r} \left(\frac{B}{2} y_{xx}^2 + \frac{T}{2} y_x^2 + \frac{\kappa}{2} y^2 - py - E_a \right) \mathrm{d}x, \quad (1)$$

where $(.)_x = \mathrm{d}(.)/\mathrm{d}x$, and the limits of integration $s_{l,r}$ define the left and right boundaries of the bleb, which are possibly dynamic. The various terms in the integrand denote, respectively, the bending energy of the membrane with flexural rigidity B, the work done by the in-plane membrane tension T, the binding energy of the adhesive bonds between the membrane and the cortex with spring constant κ, the work done by the cytoplasmic pressure p, and finally the adhesion energy between the membrane and the cortex. For consistency, the spring constant κ must be related to the adhesion energy E_a by $\kappa = 2E_a/l_c^2$, with l_c the maximum length of the membrane-cortex adhesion bond, with the condition that when $y(x) \geqslant l_c$, the adhesion bond at x breaks. The Euler-Lagrange equation derived from (1) for the shape of the bleb is then given by

$$By_{xxxx} - Ty_{xx} + \kappa y H[1 - y/l_c] - p = 0, \quad (2)$$

where $H[a] = 1, a \geqslant 0; H[a] = 0, a < 0$ is the Heaviside function. In general, the cytoplasmic pressure p is non-uniform owing to local variations in the cortical contractility, and due to the healing of the actin cortex after the bleb is formed. Here, we assume that local cortical contraction is the main contribution to the change in pressure and bleb formation consistent with observations of the non-equilibration of local hydrostatic pressure during cell blebbing and the fact that the actomyosin cortex behaves as a active poroelastic network whose contractility leads to an increase in pressure [2,13,14]. We prescribe the pressure as a localized traveling pulse given by

$$p(x,t) = \Pi \exp\left(-\frac{(x - v_\pi t)^2}{x_\pi^2} \right), \quad (3)$$

where Π, v_π, and x_π denote the magnitude, traveling speed, and width of the pulse, respectively. This form decouples actin reformation in the bleb from the changes of cortical contractility, a constraint that we will relax later on. If $v_\pi > 0$, the pressure variations as well as the bleb boundaries $s_{l,r}$ are time dependent.

Completing the formulation of the problem for the formation and dynamics of a bleb, the boundary conditions associated with eq. (2) are

$$y|_{s_{l,r}} = y_x|_{s_{l,r}} = 0 \quad (4)$$

as well as

$$\frac{B}{2}(y_{xx})^2|_{s_l} - E_a = -\mu \left(\frac{\mathrm{d}s_l}{\mathrm{d}t} - v_{H-} \right) \quad (5)$$

for the left boundary and

$$\frac{B}{2}(y_{xx})^2|_{s_r} - E_a = \mu \left(\frac{\mathrm{d}s_r}{\mathrm{d}t} + v_{H+} \right) \quad (6)$$

for the right boundary, where v_{H-} and v_{H+} are the active cortical healing speeds at the left and right boundaries of the bleb. These conditions effectively assume that the dominant dissipation mechanisms are associated with the movement of the contact lines, with μ the associated dynamic viscosity, and follow by balancing the variational derivative of the energy in eq. (1) with the relative velocity of the contact line due to passive mechanical forcing.

Our model equations can be made dimensionless by introducing a characteristic length scale $\sqrt{B/T}$, velocity scale T/μ, and energy scale B so that (2)–(6) read

$$y_{xxxx} - y_{xx} + KyH[1 - y/y_c] = P \exp\left(-\frac{(x - v_p t)^2}{x_p^2} \right), \quad (7)$$

$$y|_{s_{l,r}} = y_x|_{s_{l,r}} = 0, \quad (8)$$

$$\frac{1}{2}(y_{xx})^2|_{s_l} - J = -\left(\frac{\mathrm{d}s_l}{\mathrm{d}t} - v_{h-} \right), \quad (9)$$

$$\frac{1}{2}(y_{xx})^2|_{s_r} - J = \left(\frac{\mathrm{d}s_r}{\mathrm{d}t} + v_{h+} \right). \quad (10)$$

with the dimensionless parameters $J, K, y_c, P, x_p, v_p, v_{h\pm}$ listed in table 1. As stated earlier, in general, $P = P(v_p, v_{h\pm})$, although we will start by assuming that P is not dependent on the contractility or rate of healing.

Table 1: Dimensionless parameters in the model described by eqs. (7)–(10) and their values.

Symbol	Description	Dimensional description	Value
J	membrane-cortex adhesion energy	E_a/T	1
K	membrane-cortex spring constant	$\kappa B/T^2$	5000
y_c	critical length of membrane-cortex spring	$l_c/\sqrt{B/T}$	0.02
P	magnitude of the cytoplasmic pressure	$\Pi\sqrt{B/T^3}$	100–150
x_p	width of the pressure pulse	$x_\pi/\sqrt{B/T}$	1–10
v_p	speed of the pressure pulse	$\mu v_\pi/T$	0–20
$v_{h\pm}$	cortex-membrane healing speed	$\mu v_{H\pm}/T$	0–20

Physiologically, the material parameters J, K, and y_c are properties of adhesion molecules such as the Ezrin, Radixin and Moesin (ERM), proteins which are known to be key regulators of membrane-cortex interactions and signaling [15]. Thus, modifying the density of these ERM proteins in a cell will change the value of J, whereas modifying the sequence of the proteins may change their adhesion strength and rest length and hence K and y_c, respectively. On the other hand, the parameters related to the localized traveling pressure pulse, P, x_p, and v_p are governed by the actomyosin contractile activity in the cortex; for example, modifying the motor density affects both P and x_p whereas modifying the actin and actin crosslinker density changes P, x_p, and v_p. Finally, the healing speed $v_{h\pm}$ is governed by the rate of actin polymerization in the cortex. For our calculations, we assume the parameter values as listed in table 1, chosen to correspond to physiological values of $B \approx 10^{-19}$ J [13], $T \approx 10^{-6}$ N/m [13], $\mu = 10^{-2}$ Pa s, $E_a \approx 10^{-6}$ N/m, $\kappa \approx 10^{11}$ N/m^3, $l_c \approx 10^{-9}$ m, $\Pi \approx 100$ Pa, $x_p \approx 10^{-6}$ m, and the speeds v_p and $v_{h\pm} \in [0\text{–}10^{-4}]$ m/s.

To understand the behavior of the solutions to eqs. (7)–(10), we solve them numerically with initial conditions $s_r - s_l = 2$ (10^{-7} m in dimensional terms) and $y(x, t = 0) = 0$ for all x, using a second-order centered finite difference scheme in space and a forward Euler finite difference scheme in time. The time-step and the grid-size used are $\mathrm{d}t = 1 \times 10^{-4}$ and $\mathrm{d}x = 0.025$, respectively.

Results and discussion. –

Stationary blebs. In the static case when $v_p = v_{h\pm} = 0$, we study the nucleation and growth of a bleb as a function of the scaled pressure magnitude P and its spatial extent x_p. A bleb forms when membrane-cortex adhesive bonds are broken over a finite length, *i.e.*, $y \geqslant y_c$ for some $x \in (s_l, s_r)$. The phase diagram of stationary bleb nucleation in $P - x_p$ space is shown in fig. 1, with a phase boundary for bleb formation given by the curve $x_p \sim (P - P_0)^{-\alpha}$, in terms of a critical pressure P_0 and exponent α, which depends on the membrane flexural rigidity B. We find that $\alpha \to 1$ when $x_p \gg 1$, or equivalently, $B/T \ll x_\pi^2$ in dimensional terms, consistent with prior predictions [13]. In this limit, a scaling theory [13] also predicts that the critical pressure for bleb nucleation $P_0 = 2J/y_c$, a relation we also validate numerically (fig. 1, inset). Sample bleb shapes shown in fig. 1 confirm that both the width and the height of a stationary bleb increase with P and with x_p, as expected. We note the shapes of the blebs are less circular than actual cellular blebs; this is a reflection of our assumption of a minimal Cartesian geometry and small membrane curvatures.

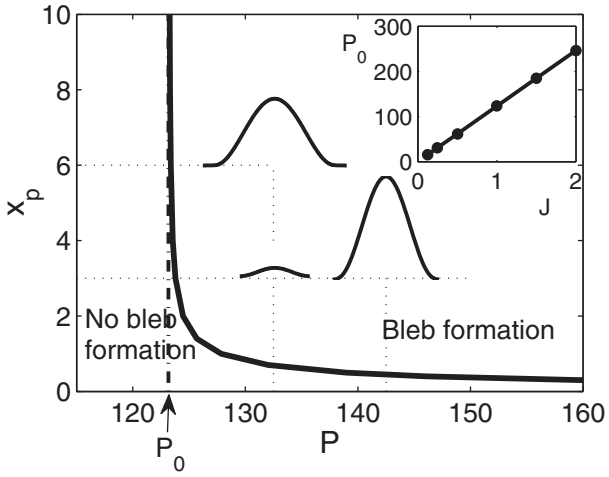

Fig. 1: Phase diagram of stationary bleb formation when $v_p = v_{h\pm} = 0$. Critical values of the pressure width x_p and the pressure magnitude P necessary for bleb formation are found to obey $x_p \sim (P - P_0)^{-\alpha}$ with $P_0 = 123.2$ and $\alpha = 0.59$. When only large values of $x_p > 3$ are considered (where bending energy can be neglected), the exponent approaches unity, namely $\alpha = 0.73$, as previously predicted [13]. The inset shows numerically calculated P_0 as a function of adhesion energy J with y_c kept constant. These numerical results agree well with the prediction $P_0 = 2J/y_c$. Several bleb shapes are also shown.

If we now let $v_{h\pm} > 0$ but keep $v_p = 0$, we observe that a bleb grows and equilibrates into an asymmetric shape (except when $v_{h+} = v_{h-}$ in which case it grows into a symmetric shape). Traveling blebs do not result from asymmetric cortical healing because the intracellular pressure is decoupled from cortical healing in this first model. When we relax this assumption later, we find that traveling blebs can indeed be sustained by asymmetric healing alone.

Traveling blebs. We now consider the case $v_p > 0$ and $P > P_0$ when blebs become non-stationary. For convenience, we will set $v_{h+} = 0$ and henceforth talk only of the relative healing speed $v_h = v_{h-}$. A sample numerical calculation of a traveling bleb is shown in fig. 2(a), (b), obtained by solving eqs. (7)–(10) for parameter values that allow for bleb nucleation. We see that a bleb first grows and moves in the direction of v_p; its shape eventually equilibrates and it travels at a constant speed given by v_p. However, not all traveling blebs can be sustained. In some instances, blebs cannot be formed or retract as they travel, even if $P > P_0$. The traveling bleb decays when either i) v_h is large, so that the trailing edge catches up with the leading edge of the bleb, or ii) v_p is large so that the leading edge has a tearing rate that lags behind the location of the pressure pulse. To understand this, we consider the boundary conditions eqs. (7)–(10) in a frame moving with speed v_p. We see that increasing v_p has the same effect as increasing the adhesion energy at the leading edge while increasing v_h has the same effect as increasing the adhesion energy at the trailing edge. Since a bleb can be sustained at equilibrium only when $P > P_0$, where P_0 is an increasing function of the adhesion energy J, a high value of either v_p or v_h will shift P_0 to a larger value, *i.e.*, $P_0 \sim 2(J + v_{p,h})/y_c$, by such an extent that the bleb eventually decays. In other words, there is a critical value of the healing speed $v_{p,h} \sim P - 2J/y_c$ above which blebs become extinct. These results are summarized in fig. 2(c), where we show two types of non-stationary blebs in the 3-dimensional phase space of P, v_p, and v_h, those that travel and those that decay.

For steady traveling blebs, our numerical simulations show that their speed is v_p is independent of v_h, deviating only in the initial stages of bleb growth. Furthermore for a given traveling speed, the shape of the bleb is determined by v_h; a symmetric bleb exists only when $v_p = v_h/2$. To understand this, we consider eqs. (7)–(10) in a moving frame with speed v_p. Then the boundaries move at speeds $\mathrm{d}s_l/\mathrm{d}t = -\left(y_{xx}\right)^2/2|_{s_l} + J - v_p + v_h$ and $\mathrm{d}s_r/\mathrm{d}t = \left(y_{xx}\right)^2/2|_{s_r} - (J + v_p)$ leading to a traveling bleb with speed v_p and boundary curvatures $\left(y_{xx}\right)^2/2|_{s_l} = J - v_p + v_h$ and $\left(y_{xx}\right)^2/2|_{s_r} = J + v_p$. We see that the bleb shape is symmetric when $v_p = v_h/2$, and confirmed by numerical simulations. Our assumption of cortical healing only along the bleb edges cannot capture the observed crumpling of the bleb membrane on retraction as we do not have a cortex along the entire blabbed membrane. However, our minimal model is sufficient to capture the qualitative trends in both the growth rates and traveling speeds.

The role of a non-local pressure. In eq. (7), we assumed that the localized perturbation for the pressure field is independent of other variables. In reality, it is coupled to the cortical contraction and healing as well as the shape of the cell membrane, as suggested by many experiments [2]. To account for this coupling, we consider

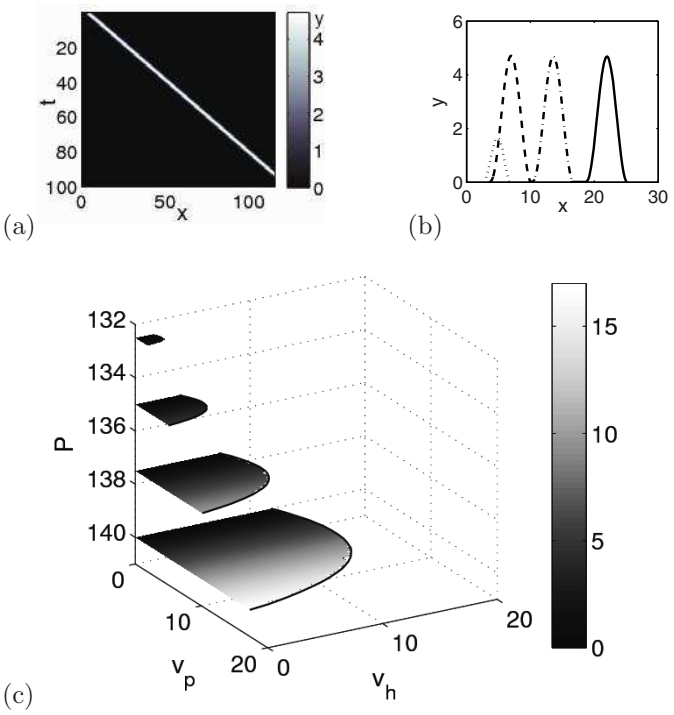

Fig. 2: (a) Kymograph showing a traveling bleb obtained from eqs. (7)–(10) with $v_p = 1.2$ and $v_h = 0.6$ showing that the traveling speed is constant; (b) Snapshots of instantaneous bleb shapes at $t = 1$ (dotted line), $t = 2.5$ (dashed line), $t = 8$ (dash-dotted line), and $t = 15$ (solid line). The parameter values used were $P = 130.8$, $x_p = 9.0$, $v_p = 1.2$, $v_h = 0.6$ and the remaining parameter values as listed in table 1. (c) Phase diagram demarcating steadily traveling and decaying phases in terms of the speed of pressure change v_p, speed of cortical healing v_h, and magnitude of pressure pulse P. Traveling regimes (shaded regimes) for $P = 132.5$, 135, 137.5, and 140 are plotted. The traveling speed of a bleb is indicated by the grayscale. The solid lines mark the boundaries between the two phases on the P planes. When P is increased, the boundary between the steadily traveling and decaying phases is shifted outwards.

the interaction of the intra- and extra-cellular fluid with the cell membrane and solve for the pressure field instead of prescribing it as an independent parameter. For relative simplicity, we assume that the other parameters associated with local cortical contraction and actin reformation, namely v_p, x_p, and v_h, remain fixed. In the context of this minimal hydrodynamic coupling model, we consider a two-dimensional cell immersed in an incompressible viscous fluid, with the same viscosity as the cytoplasm, and enclosed by an elastic membrane uniformly adhered to a permeable but rigid actin cortex through soft Hookean springs; a schematic of the model is shown in fig. 3.

Initially, the cell membrane and the cortex are assumed to be circular, with the membrane (cell) given by $\mathbf{r}_m = r_{m0}\hat{\mathbf{r}}$ and the rigid cortex given by $\mathbf{r}_c = r_{c0}\hat{\mathbf{r}}$. The membrane-cortex adhesive springs are uniformly distributed and uniformly stretched. This configuration gives rise to a uniform positive intracellular pressure. Next, we

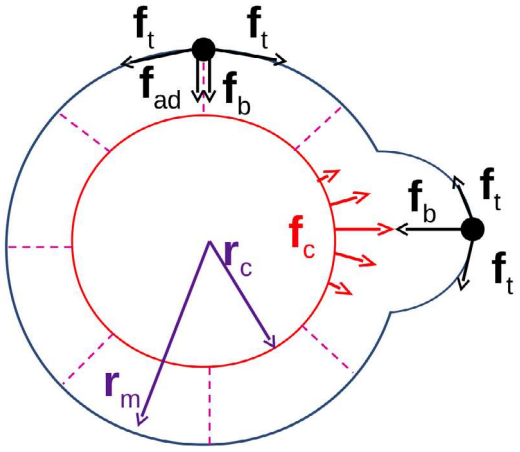

Fig. 3: (Color on-line) Schematic of the model incorporating non-local pressure. The position of the cell membrane $\mathbf{r}_m$ is solved from eqs. (12)–(15) with the forces due to membrane bending $\mathbf{f}_b$, membrane tension $\mathbf{f}_t$, membrane-cortex adhesion $\mathbf{f}_{ad}$ as shown. The inner circle of radius $\mathbf{r}_c$ denotes the cortex contracting with $\mathbf{f}_c$, and the dashed lines denote membrane-cortex adhesion.

assume that there is a slow global cortical contraction of the cell prescribed as $r_c(t) = r_{c0}\,[1 - G\,(1 - \exp(-t/\tau))]$ where G is the magnitude of global contraction and $1/\tau$ characterizes the speed of contraction. This global contraction generates a high uniform intracellular pressure that nucleates and expands a bleb when the active cortical contractive body force

$$\mathbf{f}_c(\theta, t) = L \exp\left[-A\left(1 - \cos\left(\theta - \frac{v_c t}{r_{c0}}\right)\right)\right]\hat{\mathbf{r}}, \qquad (11)$$

of magnitude L and size $\sim 1/A$, translating with speed v_c in the angular direction becomes large enough.

The presence of a localized body force $\mathbf{f}_c$ results in a non-uniform pressure field $p(\mathbf{r})$ and velocity field $\mathbf{u}(\mathbf{r})$ in the fluid, which can be deduced from the two-dimensional scaled Stokes equation and the equation of continuity

$$\nabla p = \nabla^2 \mathbf{u} + \mathbf{f}, \qquad (12)$$

$$\nabla \cdot \mathbf{u} = 0, \qquad (13)$$

where f is the total body force due to cortical contraction and membrane motion. We parameterize the cell membrane in the deformed configuration $\mathbf{r}_m(\zeta) = (x(\zeta), y(\zeta))^{\mathrm{T}}$ with $\zeta = [0, L_m]$ where L_m is the perimeter of the membrane. The motion of the membrane at position $\mathbf{r}_m$ is determined from the no-slip boundary condition imposed on the Stokes equation, *i.e.*,

$$\mathbf{u}_m = \frac{\mathrm{d}\mathbf{r}_m}{\mathrm{d}t}. \qquad (14)$$

The permeable rigid cortex that supports the cell membrane is assumed to be in a position such that at any time t, the net force experienced by the cortex is zero.

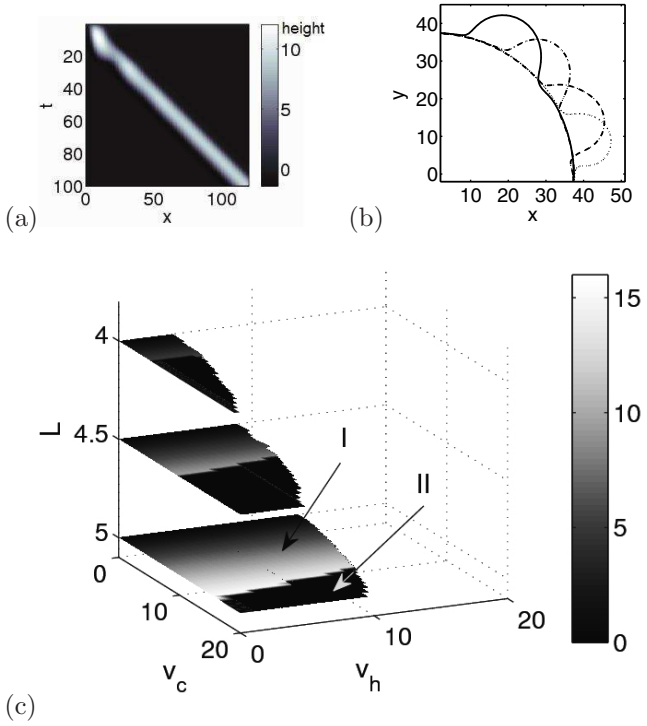

Fig. 4: (a) Kymograph showing a traveling bleb obtained from the Stokes model, with $v_c = 1.2$ and $v_h = 2.0$; (b) snapshots of instantaneous bleb shapes at $t = 2$ (dotted line), $t = 12$ (dashed line), $t = 22$ (dash-dotted line) and $t = 32$ (solid line). The parameter values used were $J = 1$, $K = 20$, $L = 4$, $A = 400$, $\tau_r = 0.25$, $v_c = 1.2$ and $v_h = 2.0$. (c) Phase diagram demarcating steadily traveling and decaying phases in terms of the speed of the localized contraction v_c, speed of cortical healing v_h, and magnitude of the local contractile force L. Traveling regimes (shaded regimes) for $L = 4$, 4.5, and 5 are plotted. A bleb is successfuly formed only when $L > 3.35$. The traveling speed of a bleb is indicated by the grayscale. Two traveling regimes are identified: i) a regime in which the traveling speed equals v_c (regime I characterized by low v_c) and ii) a regime in which the traveling speed is independent of v_c but is dependent on v_h (regime II characterized by high v_c). In the v_h-dependent regime, the traveling speed of a bleb is low but increases with increasing v_h. As v_c further increases, this v_h-dependent regime gets narrower and eventually vanishes at a high enough v_c. When L is increased, the boundary between the steadily traveling and decaying phases is shifted outwards.

Furthermore, a spring is assumed to break if the spring energy exceeds the membrane-cortex adhesion energy J (*i.e.*, if the length of the spring is greater than the critical length y_c); this detachment of membrane from the cortex results in the nucleation of a bleb. The total body force $\mathbf{f}(\mathbf{r})$ in eq. (12) is the sum of the forces from membrane bending, membrane tension, membrane-cortex adhesion, and cytoskeletal contraction, *i.e.*, and is given by

$$\mathbf{f}(\mathbf{r}) = \int_0^{L_m} [\mathbf{f}_b(\mathbf{r}_m) + \mathbf{f}_t(\mathbf{r}_m) + \mathbf{f}_{ad}(\mathbf{r}_m)]\,\delta(\mathbf{r} - \mathbf{r}_m)\,\mathrm{d}\zeta + \int_0^{L_c} \mathbf{f}_c(\mathbf{r}_c)\delta(\mathbf{r} - \mathbf{r}_c)\,\mathrm{d}\zeta, \qquad (15)$$

where $\mathbf{r}_c = \mathbf{r}_c(\zeta)$, L_c is the perimeter of the cortex and $\delta(\mathbf{r})$ is the two-dimensional Dirac delta function. In terms of the bending energy density $E_b = \gamma^2/2$ with curvature $\gamma = (x'y'' - y'x'')(x^2 + y^{'2})^{-3/2}$, the stretching energy density $E_t = \epsilon^2/2$ with strain $\epsilon = \sqrt{x'^2 + y'^2} - 1$, and the membrane-cortex spring constant K, the bending force, tensile force, and adhesive force can be evaluated in a straightforward way. We then use a boundary integral method with regularized Stokeslets [16] to solve the resulting equations eqs. (12)–(15), while the shape of membrane is determined using a forward Euler scheme.

Then bleb growth and dynamics follows by considering membrane-cortex detachment as a function of the cortical pressure, and tracking the bleb boundaries until membrane-cortex adhesion reformation, as dictated by eq. (8). We set the membrane-cortex adhesion and reformation to start at one boundary at a time τ_r after local cortical contraction occurs to prevent membrane-cortex adhesion immediately after initial membrane-cortex detachment and allow for bleb growth; τ_r thus determines the initial patch size $s_r - s_l|_{t=0}$ in eqs. (8)–(10) in nucleating the bleb.

Our non-local model also leads to steadily traveling blebs as shown in fig. 4(a), (b). Here, a bleb travels along with the local contraction speed v_c. In fig. 4(c), we show the region in phase space spanned by v_c and v_h for steadily propagating blebs and find two regimes. In regime I, shown in fig. 4(c), the speed of a bleb $v_b = v_c$, in good agreement with the linear model. In regime II, shown in fig. 4(c), the bleb speed depends on the speed of the the healing edge v_h. This occurs when the localized contractile body force is relatively small but its speed v_c is relatively large. For a given rate of edge healing v_h, the transition from regime I to regime II takes place when the contraction speed v_c is so high that the bleb lags behind cortical contraction and the process is dominated by healing.

Conclusion. – Our minimal description of the many phenomena associated with the onset, growth, dynamics, and extinction of blebs takes the form of a simple theory for the active deformations of a thin membrane partially attached to a substrate, captured in eqs. (7)–(10). Bleb growth and motion are determined by the dynamics of detachment of the cell membrane from the underlying actin cortex through the competition between the membrane bending energy and the membrane-cortex adhesion energy, coupled through a localized pressure term that models cortex contractility. When the pressure pulse is time independent, a bleb may grow and equilibrate into a stationary bleb. However, as the cytoplasmic pressure induced by local cortical contraction becomes dynamic, so does the bleb. When the pressure pulse associated with cortical contraction is independent of membrane deformation, the resulting linear theory is consistent with and complements earlier scaling predictions [13], while characterizing the formation and motion of blebs in terms of an experimentally relevant phase diagram.

We also consider a more complete theory where the contractility generated fluid pressure is coupled to membrane deformation through flow while also accounting for the cortical healing dynamics. We find that when local contraction dominates healing and the relative contribution to the pressure from hydrodynamic causes is small, the uncoupling of pressure from the other variables is reasonable. However, when the contractile forces are relatively small, we get active blebbing waves that persist because of a combination of passive hydrodynamics and active contractility for a moving boundary problem, consistent qualitatively with experiments. Our study sets the stage for bleb driven motility, wherein asymmetric forces associated with polarized blebbing can lead to the motion of whole cells when coupled with the dynamics of adhesion.

* * *

We thank Mike Sheetz for discussions, and the Harvard Kavli Institute for Nanobio Science and Technology, the MacArthur Foundation and the National University of Singapore for support.

REFERENCES

[1] Blaser H. *et al.*, *Dev. Cell*, **11** (2006) 613.
[2] Charras G. *et al.*, *Nature*, **435** (2005) 365.
[3] Charras G. T. and Paluch E., *Nat. Rev. Mol. Cell. Biol.*, **9** (2008) 730.
[4] Langridge P. D. and Kay R. R., *Exp. Cell Res.*, **312** (2006) 2009.
[5] Yoshida K. and Soldati T., *J. Cell Sci.*, **119** (2006) 3833.
[6] Wolf K. *et al.*, *J. Cell Biol.*, **160** (2003) 267.
[7] Maugis B. *et al.*, *J. Cell Sci.*, **123** (2010) 3884.
[8] Tinevez J.-Y. *et al.*, *Proc. Natl. Acad. Sci. U.S.A.*, **106** (2009) 18581.
[9] Sahai E. and Marshall C. J., *Nat. Cell Biol.*, **5** (2003) 711.
[10] Friedl P. and Wolf K., *Nat. Rev. Cancer*, **3** (2003) 362.
[11] Young J. and Mitran S., *J. Biomech.*, **43** (2010) 210.
[12] Strychalski W. and Guy R. D., to be published in *Math. Med. Biol.* (2012) doi:10.1093/imammb/dqr030.
[13] Charras G. T. *et al.*, *Biophys. J.*, **94** (2008) 1836.
[14] Charras G. T. *et al.*, *J. Cell Sci.*, **122** (2009) 3233.
[15] Fehon R. G., McClatchey A. and Bretscher A., *Nat. Rev. Mol. Cell Biol.*, **11** (2010) 674.
[16] Cortez R., *SIAM J. Sci. Comput.*, **23** (2001) 1204.